Resonant light scattering by small coated nonmagnetic spheres: magnetic resonances, negative refraction, and prediction

Cheng-Wei Qiu[1,*] and Lei Gao[2]

[1]*Department of Electrical and Computer Engineering, National University of Singapore, 4 Engineering Drive 3, Singapore 117576*

[2]*Jiangsu Key Laboratory of Thin Films, Department of Physics, Suzhou University, Suzhou 215006, China*

**Corresponding author: eleqc@nus.edu.sg*

Received May 28, 2008; revised August 4, 2008; accepted August 5, 2008;
posted August 12, 2008 (Doc. ID 96566); published September 26, 2008

Light scattering of individual coated nonmagnetic spherical particles and effective parameters for a collection of such inclusions are studied at terahertz frequencies, with the emphasis on the conditions of achieving resonant light scatterings, induced magnetic resonance, and negative refraction. Moreover, the prediciton of those critical conditions is proposed. Different core–shell combinations aiming at inducing magnetic resonances are investigated, including plasmonic metamaterials and polar crystals. It is shown that the resonant scattering is controllable with fine adjustment of the core–shell ratio, varying from enhancement to suppression in the scattering drastically. Embedding identical coated nanospheres in a matrix, the polarizability and effective medium parameters of the bulk are examined to give better understanding of unusual scatterings and their predictions. The resonances in electric and magnetic dipole approximation for such a bulk medium are presented.
© 2008 Optical Society of America
OCIS codes: 250.5403, 290.1350, 260.2030, 260.2110, 260.3090.

1. INTRODUCTION

Light scattering by small particles is a fundamental topic in classical electrodynamics [1–3]. This topic has attracted intensive attention owing to its academic importance and wide potential in many modern applications, e.g., for cloaking [4–6], field concentration for nanopatterning [7], surface-enhanced Raman scattering [8], and plasmon resonance coupling in nanorods [9]. The problem of light scattering by spherical particles has an exact solution by the Mie theory [1]. The investigations of the near-field energy flux [10,11] and far-field quantities, such as scattering cross sections near the plasmon resonances [12], have been carried out for single spheres. Exotic light scattering in a single sphere will arise for weakly dissipative materials [13] or nondissipative anisotropic materials [14] near plasmon resonance. Note that there exist two correlated processes: transformation of incident light to localized plasmons, resulting in the dissipative damping, and transformation of localized plasmons into scattered light, leading to radiative damping. Owing to the radiative damping, the scattering has finite values even at exact plasmon resonances. However, Rayleigh scattering approximation is valid only when this radiative damping is negligibly smaller than the dissipative damping. If the radiative damping becomes dominant, anomalous scattering then occurs instead of Rayleigh scattering, which results in giant optical resonances and enhanced scattering cross sections.

In a broad sense, the resonant scattering may be viewed in terms of the constructive scattering resulting in the enhancement and the destructive scattering resulting in the suppression. Despite the recent research progress in near-field interaction with novel artificial composites such as plasmonic metamaterials, it would be necessary to theoretically characterize the resonant far-field diagrams. In the present paper, we focus on the role of the core–shell ratio in the resonant scattering in the far zone induced by a distributed coated system. As for suppression, the cloaking technique has received increasing attention since the object with the cloak appears transparent to the external illumination. However, the design of cloaking materials to achieve exact invisibility requires the coating to be inhomogeneous and/or anisotropic [5,15,16]. A central concern is how to realize such inhomogeneous materials and control the tensorial elements in anisotropic materials independently.

In our previous work, enhanced scatterings for coated thin wires has been studied [17,18] by the use of plasmonic materials. Along with work on conjugate [19] and plasmonic [20] materials in slab and tube configurations, unusual wave tunneling and scattering have been well documented. Now, we further extend the study of the resonant far-field scattering to not only an individual inclusion of a coated nanosphere but also to an ensemble. Although some reports have discussed the Mie resonances associated with negative refractive metamaterials [21–23], our work is easy to differentiate from those works since coated systems may be associated with interface resonance [18], which stems from a different mechanism than that of a single sphere. Negative refractive in-

 © 2008 Optical Society of America

dex was achieved by coated nonmagnetic spheres [24]. However, how to manipulate and predict those suppressed or enhanced light scatterings has not been addressed clearly, and, in addition, the sensitivity of the negative index deserves further investigation. This motivates our present work in which exotic features of the resonant light scattering are discussed with physical insights. The theoretical modeling of the far-field scatterings in the presence of coated nanospheres is formulated and discussed with particular interest in the dipolar scattering and effective medium parameters. Contributions of multipoles to the far-field diagram are characterized and interpreted in terms of the polarizability of such coated systems [25]. Estimations of enhancement and suppression in scattering are explicitly proposed with the aim of understanding the physics behind such phenomena. The roles of the core–shell ratio and dispersion are investigated for not only the resonances in scattering but also the sensitivity of negative refraction. The use of dispersive materials such as polar crystals and Drude materials is fully explored in the study of resonant scattering, which provides possible guidelines of how to achieve desired scattering patterns and how to optimize the core–shell ratio of structured plasmonic devices.

2. SCATTERING BY INDIVIDUAL INCLUSIONS

It has been well understood that for a single homogeneous nanosphere, when $\epsilon=-(m+1)/m$ (the exact mth order resonance), the amplitude of scattering coefficients tends to limiting values [11]. At the resonances, the scattering cross sections will drastically increase and make the nanoscaled particles quite visible as if they were geometrically large. The process of such an increase can be pictured: (1) the incident wave is transformed into plasmonic polaritons by dissipative damping, and (2) the polaritons are inversely transformed into scatterings by nondissipative damping, which keeps the cross section finite even for the lossless case of $\mathrm{Im}[\epsilon]=0$.

Considering the schematic configuration on the right-hand side of Fig. 1, the coefficients of the scattered field in the outermost region, whose derivation can be found in [1], can be expressed as

$$a_m = \frac{\psi_m(y)[\psi_m'(n_s y) - A_m\chi_m'(n_s y)] - n_s\psi_m'(y)[\psi_m(n_s y) - A_m\chi_m(n_s y)]}{\xi_m(y)[\psi_m'(n_s y) - A_m\chi_m'(n_s y)] - n_s\xi_m'(y)[\psi_m(n_s y) - A_m\chi_m(n_s y)]}, \tag{1}$$

$$b_m = \frac{n_s\psi_m(y)[\psi_m'(n_s y) - B_m\chi_m'(n_s y)] - \psi_m'(y)[\psi_m(n_s y) - B_m\chi_m(n_s y)]}{n_s\xi_m(y)[\psi_m'(n_s y) - B_m\chi_m'(n_s y)] - \xi_m'(y)[\psi_m(n_s y) - B_m\chi_m(n_s y)]}, \tag{2}$$

$$A_m = \frac{n_s\psi_m(n_s x)\psi_m'(nx) - n\psi_m'(n_s x)\psi_m(nx)}{n_s\chi_m(n_s x)\psi_m'(nx) - n\chi_m'(n_s x)\psi_m(nx)}, \tag{3}$$

$$B_m = \frac{n_s\psi_m(nx)\psi_m'(n_s x) - n\psi_m'(nx)\psi_m(n_s x)}{n_s\psi_m(nx)\chi_m'(n_s x) - n\psi_m'(nx)\chi_m(n_s x)}, \tag{4}$$

where $x=k_0a$, $y=k_0b$, the refractive index of the shell is $n_s=\sqrt{\epsilon_2}$, and the refractive index of the core is $n=\sqrt{\epsilon_1}$. $\psi_m(z)$ and $\chi_m(z)$ are the Ricatti–Bessel functions of the first and second kind, respectively. $\xi_m(z)=\psi_m(z)-i\chi_m(z)$, and the derivative is with respect to the argument.

According to the definition of cross sections [1], we can express the total scattering cross section (Q_{sca}) and backscattering cross section (σ) as

$$Q_{\mathrm{sca}} = \frac{2\pi}{k_0^2}\sum_{m=1}^{\infty}(2m+1)(|a_m|^2+|b_m|^2), \tag{5}$$

$$\sigma = \frac{\pi}{k_0^2}\left|\sum_{m=1}^{\infty}(-1)^m(2m+1)(a_m-b_m)\right|^2. \tag{6}$$

We start to analyze the phenomena of enhancement and suppression in scattering from the polarizability theory [25] for such a spherically coated system. For a single electrically small coated sphere of TM polarization, it can be equivalently regarded as an electric dipole with an effective moment $\mathbf{p}$ and effective polarizability α_e placed at the sphere's origin. Similarly, a magnetic dipole with an effective moment $\mathbf{m}$ and effective polarizability α_m can be assumed for TE polarizations. Thus, once we have Eqs. (1) and (2) at hand, the coated nanosphere can be seen either as an electric dipole or a magnetic dipole, depending on the incidence.

The relation between the polarizability and the dipole moments can be expressed by using the external field ap-

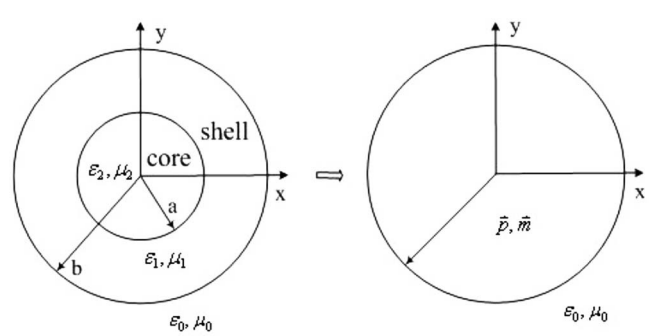

Fig. 1. Geometry for plane wave scattering by the conventional dielectric sphere covered by a plasmonic shell, which can be interpreted by dipole moments. The permeabilities in all regions are assumed to be identical to that of free space, and the permittivities are relative values.

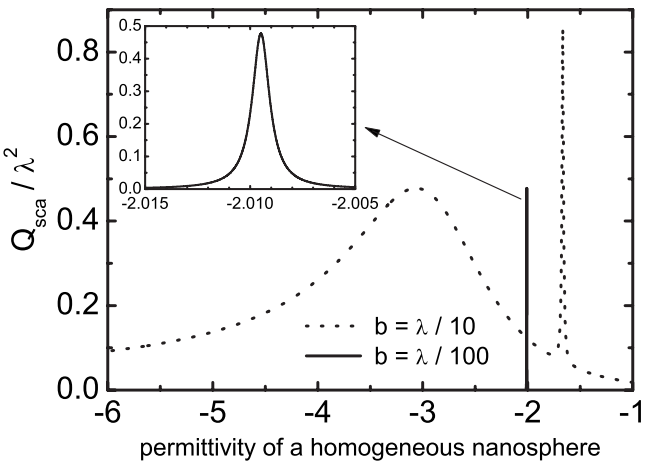

Fig. 2. Constructive scattering of a plasmonic nanosphere versus its permittivity when the materials in the core and shell are identical, i.e., $n_2=n_3$. Solid curve, $b=\lambda/100$; dashed curve, $b=\lambda/10$. The inset illustrates the variation of scattering in a fine region in the vicinity of plasmon resonance.

proach [26] for spherical cases without magnetoelectric coupling [27–29]: $\mathbf{p}=\alpha_e\mathbf{E}$ and $\mathbf{m}=\alpha_m\mathbf{H}$. $\mathbf{E}$ and $\mathbf{H}$ denote the external electromagnetic fields [30], and the polarizabilities of the coated sphere in Fig. 1 are found to be

$$\alpha_e = \frac{4\pi b^3}{\Delta}\{(\epsilon_1-1)(\epsilon_2+2\epsilon_1)-(a/b)^3[2\epsilon_1^2+\epsilon_1(1-2\epsilon_2)-\epsilon_2]\}, \tag{7}$$

$$\alpha_m = \frac{4\pi b^3}{\Delta}\{\epsilon_1(1-\epsilon_1)(a/b)^3\}, \tag{8}$$

where

$$\Delta = (\epsilon_1+2)(\epsilon_2+2\epsilon_1)-2(a/b)^3(\epsilon_1-\epsilon_2)(\epsilon_1-1). \tag{9}$$

Hence, it would be straightforward to have the condition of achieving transparency of TM polarization by requiring Eq. (7) to be zero, which actually makes the effective permittivity equal to that of free space exactly. Thus, if $\epsilon_2=4$, $\epsilon_1=-3$, and $b=\lambda/100$, the transparency will occur at $a/b\approx 0.6114$.

From Eqs. (7) and (9), one can see that the destructive interference for TM polarization requires

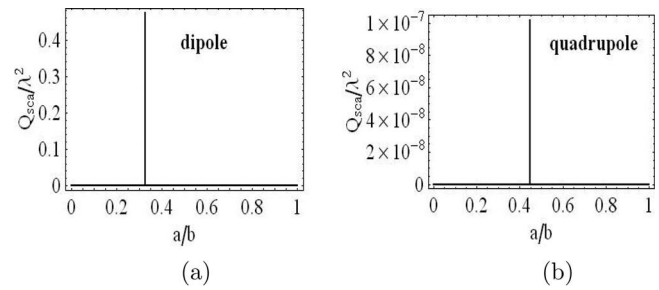

Fig. 3. Constructive scattering dominated by 2^m multipoles for the plasmonic coated nanosphere when the core sphere has $\epsilon_2=4$ and the plasmonic shell has $\epsilon_1=-3$. The outer radius is fixed at $b=0.01\lambda$.

$$a/b = \sqrt[3]{\frac{(\epsilon_1-1)(\epsilon_2+2\epsilon_1)}{2\epsilon_1^2+\epsilon_1(1-2\epsilon_2)-\epsilon_2}}, \tag{10}$$

and the constructive interference demands

$$a/b \approx \sqrt[3]{\frac{(\epsilon_1+2)(\epsilon_2+2\epsilon_1)}{2(\epsilon_1-\epsilon_2)(\epsilon_1-1)}}, \tag{11}$$

which are valid for particles of electrically small size.

Peculiar enhancement in the total scattering cross section Q_{sca}/λ^2 of a homogeneous nanosphere is first reported in Fig. 2, which is slightly shifted from the exact first-order resonance. In Fig. 2, we consider Q_{sca}/λ^2 versus the permittivity of the nanosphere at two different sizes, and only the scattering coefficient a_1 is involved in this case since b_1 is very small. It shows that the plasmonic materials that have negative permittivities at optical frequencies would have the total scattering cross section greatly enhanced. For the size of $b=\lambda/10$, the constructive bandwidth where the scattering is enhanced significantly is very wide, covering almost all regions of negative permittivity. On the contrary, when the size is further scaled downward to $b=\lambda/100$, the constructive bandwidth becomes very narrow, and the inset in Fig. 2 also shows that the maximum of the normalized scattering arises at $\epsilon\approx-2.01$ instead of the exact plasmon resonance of the first order where $\mathrm{Re}[\epsilon]=-2$.

It is interesting to see that for a normal plasmonic nanosphere used in medicine and engineering, constructive scattering will never arise at the exact plasmon resonance (e.g., the maximum for the case $b=0.01\lambda$ is at $\epsilon=-2.01$), which is always shifted toward the lower end of

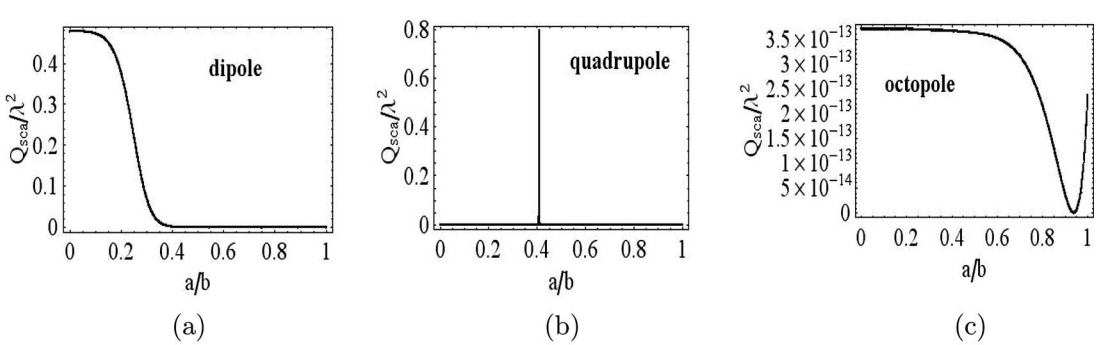

Fig. 4. Constructive scattering dominated by 2^m multipoles for the plasmonic coated nanosphere when the core sphere has $\epsilon_2=4$ and the plasmonic shell has $\epsilon_1=-3$. The outer radius is fixed at $b=0.1\lambda$.

the permittivity. Hence, the shift in resonant scattering becomes an important issue. When the size of the plasmonic nanosphere becomes larger, the shift in resonant light scattering becomes remarkable (e.g., the maximum of scattering for $b=0.1\lambda$ is at $\epsilon\approx-3$).

Therefore, it could be concluded that a small plasmonic shell coated on a given nanosphere would resonate dominantly as either a dipole, a quadrupole, or an octopole [31], depending on the selection of the plasmonic materials and the core–shell ratio. In Fig. 3, the contribution due to different multipolar terms in a coated plasmonic nanosphere is characterized. For extremely small coated nanoparticles, a proper radii ratio of inner core over outer shell would only induce constructive dipolar scattering, while the scattering due to higher-order multipoles (e.g., the quadrupolar contribution is of the order of 10^{-7}, and the octopolar contribution is of the order of 10^{-30}) are negligible as shown in Fig. 3. When the coated nanosphere is slightly larger (e.g., $b=0.1\lambda$ as in Fig. 4), it can be seen that both the dipolar and quadrupolar constructive scatterings are permissible, and one can tune the ratio of a/b to select one of them to be the dominant one. The higher-order multipoles from the octopole onward can be neglected. Such particular constructive scattering is very sensitive to the radii ratio, which may have been ignored before.

Figure 5(a) shows that the destructive and constructive scatterings only occur at their particular ratios (i.e., $a/b=0.329$ for enhancement and $a/b=0.611$ for suppression) for a very small coated nanosphere, which can be verified by the prediction schemes based on the polarizability. If the size increases to 0.1λ, the destructive scattering arises at its particular ratio of $a/b=0.53$, while the pattern of the constructive scattering is complicated. One can see that scattering is enhanced within a wide range, $0<a/b<0.405$, with magnitudes of several orders higher than other situations. At $a/b=0.405$, the scattering meets its maximum. It is interesting to note that for the particular ratio of destructive scattering for the case of $b=0.1\lambda$, the prediction schemes provided in Eq. (10) for dipolar scattering fail to work. This is because coated plasmonic nanospheres as in Fig. 5(b) resonate as neither a dipole nor a quadrupole, which complicates the prediction of the suppression and enhancement in scattering. The insets in Fig. 5 report particular ratios of a/b where the backscattered field can be suppressed.

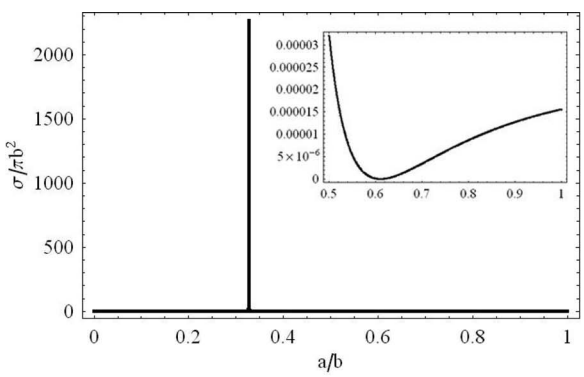

(a) $b=0.01\lambda$

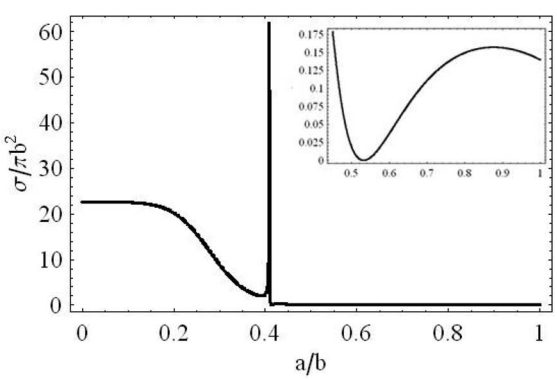

(b) $b=0.1\lambda$

Fig. 5. Normalized backscattered cross section with the inset to show the enhancement and suppression for the coated plasmonic nanosphere. The parameters in the core and shell are $\epsilon_2=4$ and $\epsilon_1=-3$, respectively.

Certain semiconductor composites such as GaAs, which follow the single-oscillator model [29,32], possess the required negative permittivity under some circumstances. It should be noted, however, that those single-oscillator models are valid only until the material undergoes a transition to a metal. After the transition, the optical parameters of the material are no longer precisely represented by single-oscillator models. Instead, the Drude model [33,34], which assumes a carrier density equal to the total valence electron density, can approximate the permittivity of metals or semiconductors after the transition:

$$\epsilon_{\text{Drude}}=1-\frac{\omega_p^2}{\omega(\omega+i\gamma)}, \tag{12}$$

where ω_p is the plasmon frequency, and the damping frequency γ is usually represented in terms of dimensionless damping parameter γ/ω_p.

In Fig. 6, we consider the backscattered radar cross section of a core sphere of radius 5 μm coated by a Drude cover of radius 10 μm. It can be seen that the presence of the damping, even though it is very small, would only drastically reduce the intensity of the resonant scattering without affecting the resonance frequency. As for the dielectric of the core sphere as shown in Fig. 6(a), there will be two resonance frequencies for a lossless Drude cover (i.e., $\omega_1=1.3$ THz and $\omega_2=2.16$ THz). By introducing the dimensionless damping of 0.01 in Fig. 6(b), the resonant backscattering at the first resonance frequency ω_1 would be significantly attenuated. Although similar attenuation occurs for the scattering at ω_2, the backscattering is still 10 times larger than that at ω_1, which plays the leading role. Hence, the effects of the damping upon the resonant scattering at different resonance frequencies are markedly different for the case of a dielectric core (medium permittivity value) when a Drude material is coated on that.

Furthermore, the case of a high-permittivity core $\epsilon_2=40$, which is conveniently available from semiconductors such as NaCl and KCl, is investigated. It is found that only one resonance frequency exists at 1.95 THz in the cases presented in Fig. 6(c), indicating that the use of a high-permittivity composite as the core may lead to interesting results. Such phenomena will be further examined and discussed in terms of effective medium theory.

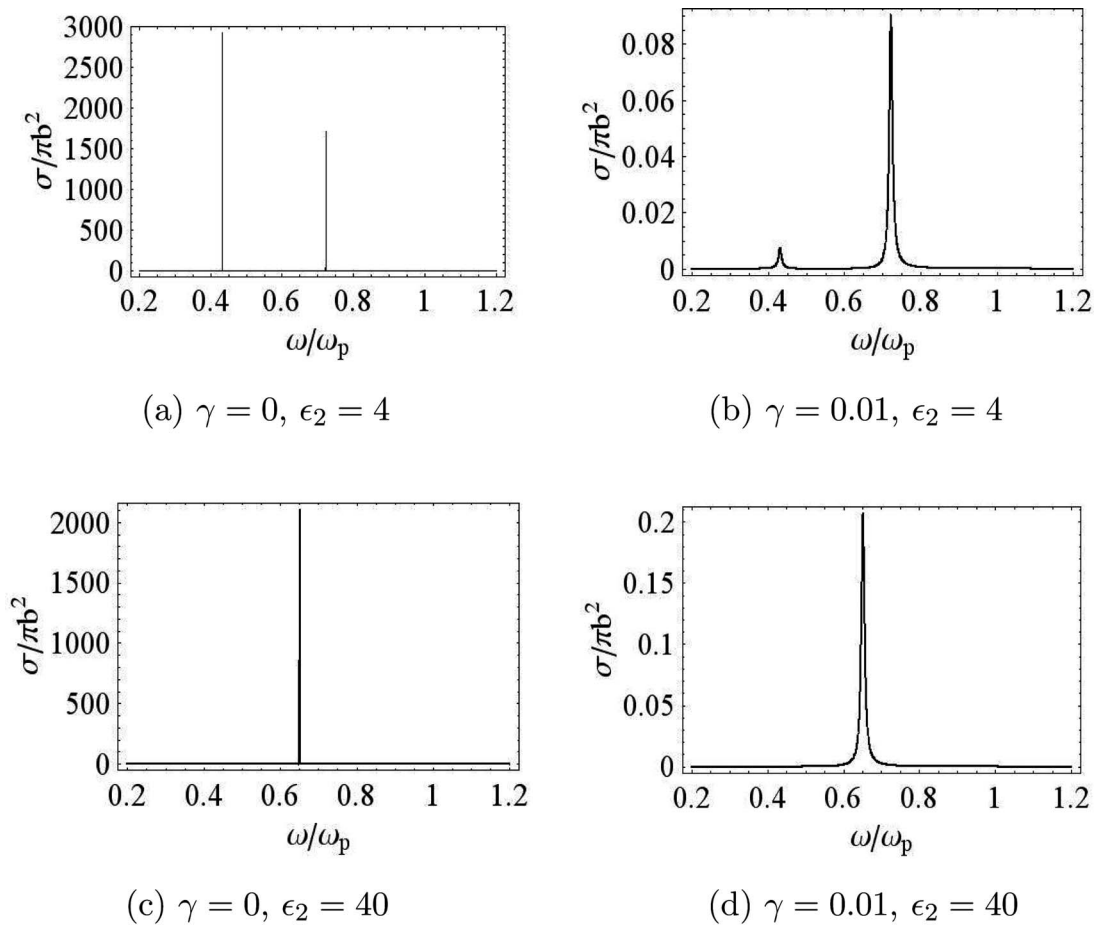

Fig. 6. Drude materials in the coating with different dielectric cores at the ratio $a/b=0.5$. The outer radius b is 10 μm, and the plasmon frequency $\omega_p=3$ THz.

The variations of backscattering versus the frequency and core–shell ratio are shown in Fig. 7 for lossless and lossy cases. The presence of loss is an inevitable consequence of the underlying resonances. Figure 7 gives a three-dimensional picture of the dependence of the constructive scattering. It is obvious that the loss in the Drude shell greatly attenuates the resonant scattering magnitudes. Even if the dimensionless damping factor is 0.01, the absolute damping frequency is still very high considering the coated sphere is operated at terahertz frequency.

Previous results show the scattering enhancement and suppression with the presence of interface polaritons related to a particular geometry of the plasmonic shell. Now, one may raise the question, would the resonant scatterings be permissible for a normal dielectric shell coated on a dielectric nanosphere? First of all, let us revisit Eqs. (7) and (9), from which one can obtain for the coefficient of the dipolar scattering

$$a_1 = -i\frac{2}{3}(k_0 b)^3 \times \frac{(\epsilon_1-1)(\epsilon_2+2\epsilon_1)-(a/b)^3[2\epsilon_1^2+\epsilon_1(1-2\epsilon_2)-\epsilon_2]}{(\epsilon_1+2)(\epsilon_2+2\epsilon_1)-2(a/b)^3(\epsilon_1-\epsilon_2)(\epsilon_1-1)}. \tag{13}$$

If the dielectric permittivity of the core ϵ_2 is conventionally positive, the permittivity of the shell ϵ_1 has to be negative in order to satisfy the physical constraint $0<a/b<1$ as discussed previously. However, there is a special case such that a/b has a physical solution even if ϵ_1 is also positive. Assuming $\epsilon_2 \gg \epsilon_1$, Eq. (13) can be represented as

$$a_1 = i\frac{2}{3}(k_0 b)^3 \frac{(1-\epsilon_1)-(a/b)^3(2\epsilon_1+1)}{(2+\epsilon_1)-2(a/b)^3(1-\epsilon_1)}. \tag{14}$$

Therefore, $0<\epsilon_1<1$ is the permissible region for a dielectric shell to achieve destructive scattering, whereas constructive scattering would be difficult to realize since the denominator of Eq. (14) can never be zero in the regime of $0<\epsilon_1<1$. Since $|a_1| \gg |b_1|$ for sufficiently small particles, only a_1 is needed in the calculation of backscattering cross sections for positive dielectric core–shell systems.

In Fig. 8, three particular ratios for destructive dipolar backscattering can be determined by $a/b = \sqrt[3]{(1-\epsilon_1)/(1+2\epsilon_1)}$ from Eq. (14) (i.e., 0.91, 0.83, and 0.69 for the solid, dashed, and dotted–dashed curves, respectively). It can be seen that there is no constructive backscattering no matter how the radii ratio is tuned in such a core–shell system. The limiting value at $a/b=1$ actually indicates that the thickness of the shell is zero and the coated system is reduced to a perfectly conducting sphere. However, if the core is made of polaritonic materials such

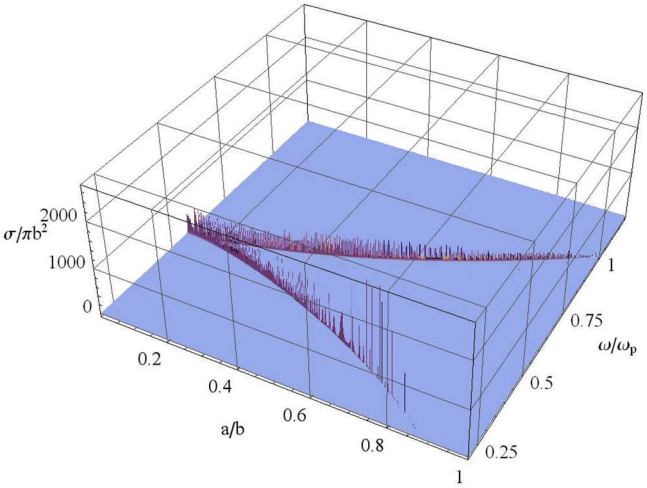

(a) $\gamma = 0$

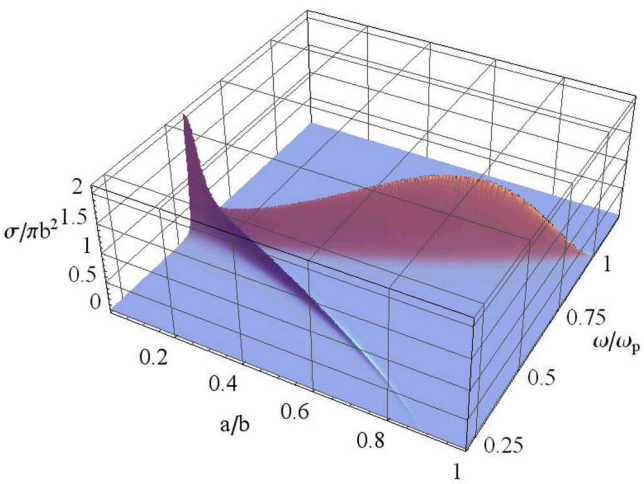

(b) $\gamma/\omega_p = 0.01$

Fig. 7. (Color online) Three-dimensional plot of the backscattering of the dielectric core $\epsilon_2=4$ coated by a Drude material whose outer radius b is 2 μm and the plasmon frequency is $\omega_p = 30$ THz.

as NaCl [35] with high permittivity within certain frequency bands, the limiting value will be slightly smaller at $a/b=1$.

3. EFFECTIVE PARAMETERS AND SENSITIVITY ANALYSIS OF THE RESONANCES

Now, let us study the structural response of an ensemble of such plasmonic coated nanospheres by considering the resonances in effective parameters.

The scattered electric and magnetic dipolar fields are proportional to the coefficients a_1 and b_1 in Eqs. (1) and (2), respectively [1]. From the dipole approximation, the effective parameters for an ensemble of coated nanospheres can be obtained [24]:

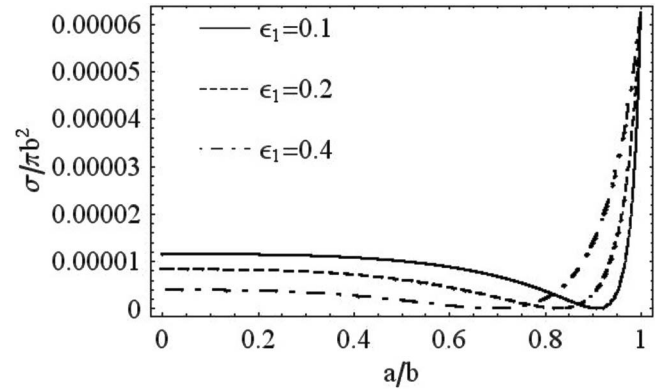

Fig. 8. Backscattering versus radii ratio for the coated sphere in which the permittivity of the core is markedly larger than that of the shell. Both layers are dielectrics and the outer radius is $b = 0.01\lambda$.

$$\epsilon_{\text{eff}} = \frac{k_0^3 + i4\pi N a_1}{k_0^3 - i2\pi N a_1}, \tag{15}$$

$$\mu_{\text{eff}} = \frac{k_0^3 + i4\pi N b_1}{k_0^3 - i2\pi N b_1}, \tag{16}$$

where N denotes the density of each effective sphere sized at a radius of b. Because of the constraints of the dilute mixing requirements for the Maxwell–Garnett formula, the filling fraction $f=4\pi N b^3/3$ cannot be large; otherwise a higher-order correction term has to be implemented [36]. It can be seen that the bulk parameters of the composited spheres depend on the materials in each layer, the radius, and the frequency if the material is dispersive.

From Eqs. (15) and (16), one can see that if the scattering coefficients a_1 and b_1 can be very large in the same frequency band, the effective permittivity and permeability become negative simultaneously. However, in most of the cases, b_1 (or the magnetic dipole) is weak especially in nanosized particles. However, both polar crystals [22] and ferroelectrics [37] can still induce the magnetic resonance due to their high permittivity in the reststrahlen region [38]. Such polar crystals include TlCl, TlBr, and GaAs [35], and the relative permittivity exhibiting phonon polaritons follows the form of

$$\epsilon_{\text{polar}}(\omega) = \epsilon_\infty + \frac{\epsilon_0 - \epsilon_\infty}{1 - (\omega/\omega_T)^2 - i(\gamma/\omega_T)(\omega/\omega_T)}, \tag{17}$$

where ϵ_0 stands for the low-frequency permittivity, ϵ_∞ is the high-frequency limit of the permittivity, ω_T is the long-wavelength transverse optical phonon frequency, and γ represents the intrinsic damping. The Lyddane–Sachs–Teller relation [39] connects the longitudinal optical phonon frequency ω_L with these parameters:

$$\frac{\omega_L^2}{\omega_T^2} = \frac{\epsilon_0}{\epsilon_\infty}. \tag{18}$$

ϵ_0 is always higher than ϵ_∞ because a longitudinal phonon has an associated electric field providing a restoring force, which means $\omega_L > \omega_T$ [40]. In the limit $\gamma \to 0$, the permittivity can increase to arbitrary positive values when the

frequency approaches ω_T from below and can decrease to arbitrary negative values approaching ω_T from above. Hence, such polar crystals could perform as either high-permittivity or plasmonic materials at particular frequency regions.

In Fig. 9, three types of dielectric core spheres are considered, ranging from normal to extremely high values of the permittivity ϵ_2. It is shown that the increasing permittivity in the core will induce magnetic resonances close to electric resonance (i.e., within $0.5\omega_p$) when the permittivity in the core goes beyond a particular valve value. In the case presented in Fig. 9, the valve of ϵ_2 is approximately 240. It is worth noting that Figs. 9(b) and 9(d) do not mean no resonances. Instead, those resonances in μ_{eff} are far off those resonances in ϵ_{eff}, which are suppressed subsequently. Surprisingly, one can find that only one electric resonance arises in the case of high-permittivity cores while two electric resonances are present for normal dielectric cores. Also, for the high-permittivity cores coated by a Drude shell, the increment in the core's permittivity hardly affects the resonant frequency in effective permittivity, but the resonant frequency in effective permeability is greatly modified. For instance, the resonant frequency in Fig. 9(f) occurs at $\omega = 36.6$ THz, and if we consider $\epsilon = 180$, the corresponding resonant frequency in effective permeability occurs at $\omega = 52$ THz.

Up to now, the resonances in ϵ_{eff} and μ_{eff} are not over-

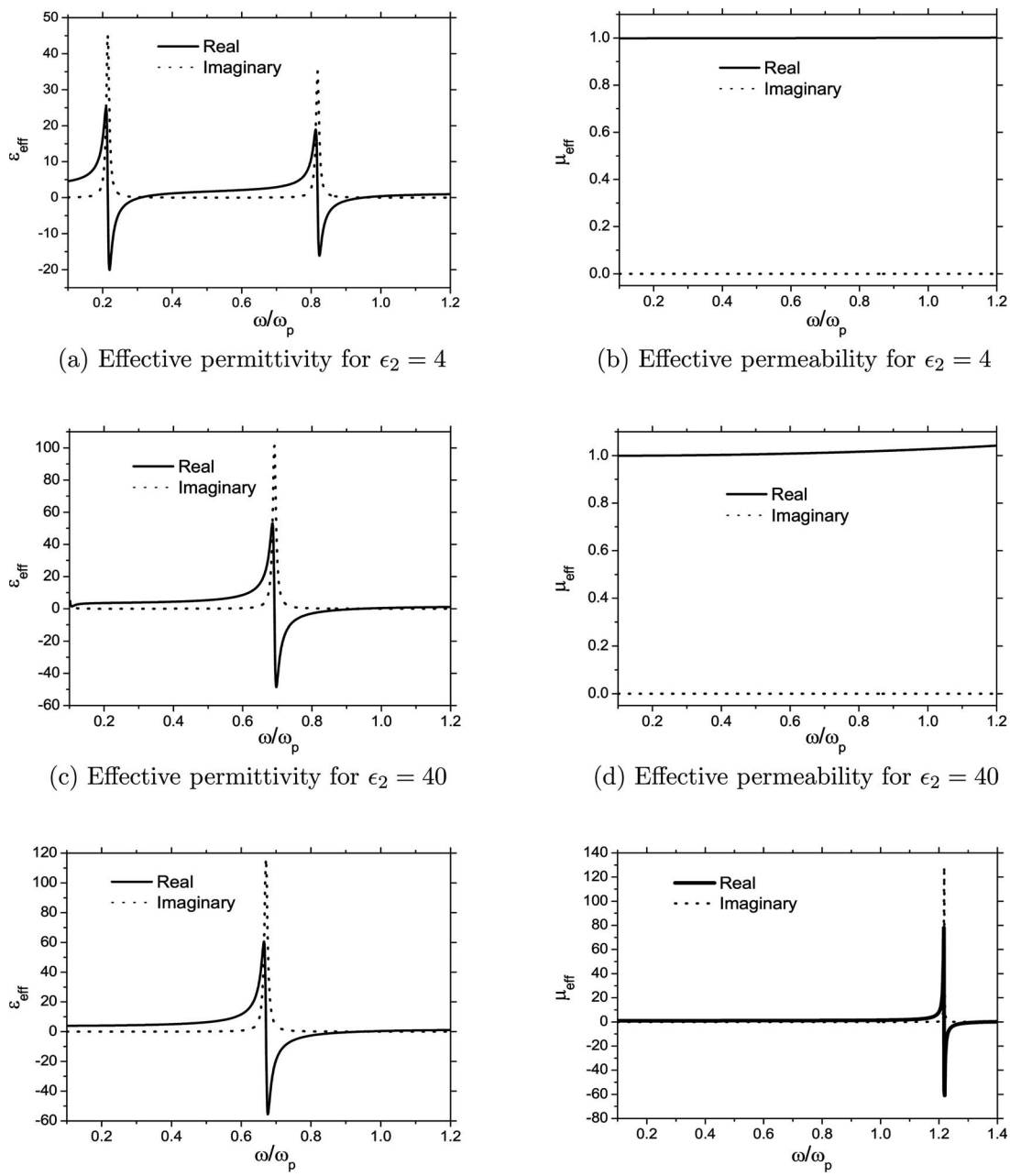

(a) Effective permittivity for $\epsilon_2 = 4$

(b) Effective permeability for $\epsilon_2 = 4$

(c) Effective permittivity for $\epsilon_2 = 40$

(d) Effective permeability for $\epsilon_2 = 40$

(e) Effective permittivity for $\epsilon_2 = 240$

(f) Effective permeability for $\epsilon_2 = 240$

Fig. 9. Effective parameters of the coated spheres with a Drude shell. $b = 2$ μm, $a = 1.6$ μm, and $\omega_p = 30$ THz. Solid (dashed) curve corresponds to the real (imaginary) part. The filling fraction is 0.5, and the dimensionless damping factor is 0.01.

lapping, which means such a collection of coated spheres is not left handed. The central concern is how to make the electric and magnetic resonances be within the same frequency band. Throughout the numerous examples considered but suppressed, it was revealed that a smaller outer size b requires a higher permittivity of the core to make the magnetic resonance close to electric resonance, provided that other parameters remain unchanged. Therefore, if the size of the particles is extremely small at several nanometers, it will be almost impossible to induce collective magnetic resonance because no natural or artificial materials can provide such high permittivity as required.

Thus, in Fig. 10, we consider the outer size $b=4$ μm for each inclusion to alleviate the requirement in the core's permittivity of polar crystals, and the inner and outer spheres are occupied by polar and Drude material, respectively. The effective refractive index n_{eff} is presented in Fig. 10, indicating that electric and magnetic resonances overlap each other within the frequency bandwidth where the real part in n_{eff} exhibits the negative sign. The parameters of the permittivity of TlCl spheres in the core are extracted from experiments [37]: $\epsilon_0=31.9$, $\epsilon_\infty=5.1$, $\omega_T=12$ THz, and $\omega_L=30$ THz.

Our sensitivity analysis reveals that there exist lower and upper bounds for the ratio a/b to achieve negative refraction at terahertz frequencies. Beyond such bounds, the real parts of the refractive index will never be nega-

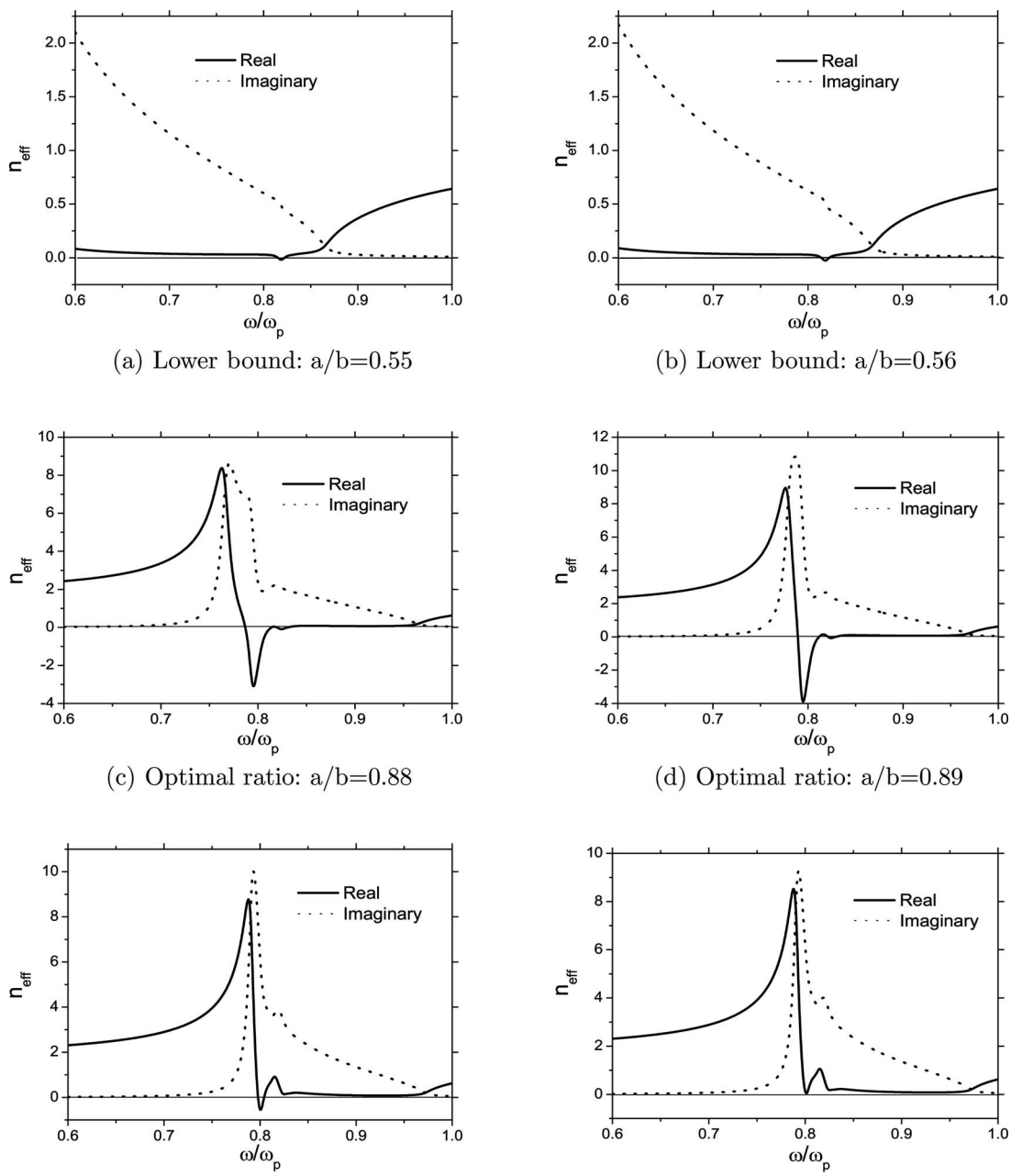

(a) Lower bound: a/b=0.55 (b) Lower bound: a/b=0.56

(c) Optimal ratio: a/b=0.88 (d) Optimal ratio: a/b=0.89

(e) Upper bound: a/b=0.904 (f) Upper bound: a/b=0.905

Fig. 10. Effective refractive index of a class of TlCl spheres coated by Drude materials. The outer radius is $b=5.2$ μm, and $\omega_p=14.4$ THz. The filling fraction is 0.5, and the dimensionless damping for both TlCl and Drude materials is 0.01.

tive. The lower and upper bounds are found to be 0.55 and 0.905, respectively. One can also conclude that in the coated system in Fig. 10, a relatively thin coating of Drude materials would be a better choice, if one wants to obtain a larger bandwidth of negative refractive indices. Figure 10(b) represents those ratios where the negative refractive indices have optimal values and frequency bandwidths. Another interesting finding is that the upper bound is very sensitive. When $a/b=0.904$, there is still a reasonably large negative-index bandwidth considering the value of ω_p. A subtle increment of 0.1% in the ratio would result in the absence of such a desired bandwidth while the whole pattern remains almost unchanged. Therefore, from the present work, the core–shell ratio is of great importance not only in a single coated nanosphere but also in a system of many coated nanospheres, though the combination of the polar crystals and Drude materials provides a possibility to achieve electric and magnetic resonances simultaneously.

4. SUMMARY

In this contribution we have studied the physics of resonant light scattering by coated nonmagnetic nanospheres and how to manipulate such constructive (destructive) scattering from the view of the core–shell ratio. A coated spherical particle that is not negligible to the wavelength can be invisible, and in the opposite limit, an extremely small nanoparticle can be visible. We have considered not only artificial plasmonic materials but also polar crystals operating in terahertz domains. Numerical examples and physical insights of such scatterings were provided and discussed. It has also been shown how the resonant scattering as well as bulky resonances depend on the core–shell ratio in each inclusion. The prediction based on the polarizability and the sensitivity of the negative index were proposed and analyzed. Thus, the scattering diagrams and effective parameters can be tailored by one more degrees of freedom, which is not available in single spheres. Since the negative value or giant positive value in the real part of the permittivity is conveniently available from the Drude model and polar crystals, those resonant light scatterings discussed here become highly applicable in the areas of medical detection and negative-index materials.

ACKNOWLEDGMENTS

C.-W. Qiu is grateful for the support from the SUMMA Foundation in the U.S. and the French–Singaporean Merlion Project. L. Gao acknowledges the National Natural Science Foundation of China (NNSFC) under grant 10674098 and the National Basic Research Program under grant 2004CB719801. We thank B. Luk'yanchuk for stimulating discussion.

REFERENCES

1. C. F. Bohren and D. R. Huffman, *Absorption and Scattering of Light by Small Particles* (Wiley, 1998).
2. J. D. Jackson, *Classical Electrodynamics*, 2nd ed. (Wiley, 1975).
3. L. D. Landau, E. M. Lifshitz, and L. P. Pitaevskii, *Electrodynamics of Continuous Media*, 2nd ed., Course of Theoretical Physics, Vol. 8 (Pergamon, 1984).
4. D. Schurig, J. J. Mock, B. J. Justice, S. A. Cummer, J. B. Pendry, A. F. Starr, and D. R. Smith, "Metamaterial electromagnetic cloak at microwave frequencies," Science **314**, 977–980 (2006).
5. S. A. Cummer, B. I. Popa, D. Schurig, D. R. Smith, and J. B. Pendry, "Full-wave simulations of electromagnetic cloaking structures," Phys. Rev. E **74**, 036621 (2006).
6. M. G. Silveirinha, A. Alù, and N. Engheta, "Parallel-plate metamaterials for cloaking structures," Phys. Rev. E **75**, 036603 (2007).
7. S. Papernov and A. W. Schmid, "Correlations between embedded single gold nanoparticles in SiO_2 thin film and nanoscale crater formation induced by pulsed-laser radiation," J. Appl. Phys. **92**, 5720–5728 (2002).
8. D. A. Weitz, T. J. Gramila, and A. Z. Genack, "Anomalous low-frequency Raman scattering from rough metal surfaces and the origin of surface-enhanced Raman scattering," Phys. Rev. Lett. **45**, 355–358 (1980).
9. K. Li, M. I. Stockman, and D. J. Bergman, "Self-similar chain of metal nanospheres as an efficient nanolens," Phys. Rev. Lett. **91**, 227402 (2003).
10. C. F. Bohren, "How can a particle absorb more than the light incident on it?" Am. J. Phys. **51**, 323–327 (1983).
11. Z. B. Wang, B. S. Luk'yanchuk, M. H. Hong, Y. Lin, and T. C. Chong, "Energy flow around a small particle investigated by classical Mie theory," Phys. Rev. B **70**, 035418 (2004).
12. M. I. Tribelsky and B. S. Luk'yanchuk, "Anomalous light scattering by small particles," Phys. Rev. Lett. **97**, 263902 (2006).
13. B. S. Luk'yanchuk and C. W. Qiu, "Enhanced scattering efficiencies in spherical particles with weakly dissipating anisotropic materials," Appl. Phys. A **92**, 773–776 (2008).
14. C. W. Qiu and B. S. Luk'yanchuk, "Peculiarities in light scattering of spherical particles with radial anisotropy," J. Opt. Soc. Am. A **25**, 1623–1628 (2008).
15. A. Hendi, J. Henn, and U. Leonhardt, "Ambiguities in the scattering tomography for central potentials," Phys. Rev. Lett. **97**, 073902 (2006).
16. J. B. Pendry, D. Schurig, and D. R. Smith, "Controlling electromagnetic fields," Science **312**, 1780–1782 (2006).
17. C. W. Qiu, H. Y. Yao, S. N. Burokur, S. Zouhdi, and L. W. Li, "Electromagnetic scattering properties in a multilayered metamaterial cylinder," IEICE Trans. Commun. **E90-B**, 2423–2429 (2007).
18. C. W. Qiu, S. Zouhdi, and Y. L. Geng, "Shifted resonances in coated metamaterial cylinders: enhanced backscattering and near-field effects," Phys. Rev. E **77**, 046604 (2008).
19. A. Alù and N. Engheta, "Pairing an epsilon-negative slab with a mu-negative slab: resonance, tunneling and transparency," IEEE Trans. Antennas Propag. **51**, 2558–2571 (2003).
20. S. B. O'Brien and J. B. Pendry, "Photonic band-gap effects and magnetic activity in dielectric composites," J. Phys.: Condens. Matter **14**, 4035–4044 (2002).
21. C. L. Holloway, E. F. Kuester, J. Baker-Jarvis, and P. Kabos, "A double negative (DNG) composite medium composed of magnetodielectric spherical particles embedded in a matrix," IEEE Trans. Antennas Propag. **51**, 2596–2603 (2003).
22. V. Yannopapas and A. Moroz, "Negative refractive index metamaterials from inherently non-magnetic materials for deep infrared to terahertz frequency ranges," J. Phys.: Condens. Matter **17**, 3717–3714 (2005).
23. R. L. Chern, X. X. Liu, and C. C. Chang, "Particle plasmons of metal nanospheres: application of multiple scattering approach," Phys. Rev. E **76**, 016609 (2007).
24. M. S. Wheeler, J. S. Aitchison, and M. Mojahedi, "Coated nonmagnetic spheres with a negative index of refraction at infrared frequencies," Phys. Rev. B **73**, 045105 (2006).
25. I. V. Lindell, A. H. Sihvola, S. A. Tretyakov, and A. J. Viitanen, *Electromagnetic Waves in Chiral and Bi-Isotropic Media* (Artech House, 1994).

26. A. H. Sihvola and I. V. Lindell, "Polarizability and effective permittivity of layered and continuously inhomogeneous dielectric spheres," J. Electromagn. Waves Appl. **3**, 37–60 (1989).
27. S. A. Tretyakov and A. J. Viitanen, "Plane waves in regular arrays of dipole scatterers and effective-medium modeling," J. Opt. Soc. Am. A **17**, 1791–1797 (2000).
28. C. W. Qiu, H. Y. Yao, L. W. Li, S. Zouhdi, and T. S. Yeo, "Backward waves in magnetoelectrically chiral media: propagation, impedance, and negative refraction," Phys. Rev. B **75**, 155120 (2007).
29. C. W. Qiu, H. Y. Yao, L. W. Li, S. Zouhdi, and T. S. Yeo, "Routes to left-handed materials by magnetoelectric couplings," Phys. Rev. B **75**, 245214 (2007).
30. A. H. Sihvola, *Effective Permittivity of Multiphase Mixtures: The Scatterer as a Two-Layer Sphere*, Rep. 19 (Helsinki University of Technology, 1987).
31. B. S. Luk'yanchuk and V. Ternovsky, "Light scattering by a thin wire with a surface-plasmon resonance: bifurcations of the Poynting vector field," Phys. Rev. B **73**, 235432 (2006).
32. E. U. Condon, "Theories of optical rotatory power," Rev. Mod. Phys. **9**, 432–457 (1937).
33. J. B. Pendry, A. J. Holden, W. J. Stewart, and I. Youngs, "Extremely low frequency plasmons in metallic mesostructures," Phys. Rev. Lett. **76**, 4773–4776 (1996).
34. H. Shin and S. Fan, "All-angle negative refraction for surface plasmon waves using a metal-dielectric-metal structure," Phys. Rev. Lett. **96**, 073907 (2006).
35. C. Kittel, *Introduction to Solid State Physics*, 7th ed. (Wiley, 1996).
36. O. Ouchetto, C. W. Qiu, S. Zouhdi, L. W. Li, and A. Razek, "Homogenization of 3D periodic bianisotropic metamaterials," IEEE Trans. Microwave Theory Tech. **54**, 3893–3898 (2006).
37. G. Burns and E. Burstein, "Dirty displacive ferroelectrics," Ferroelectrics **7**, 297–299 (1974).
38. A. D. Boardman, ed., *Electromagnetic Surface Modes* (Wiley, 1982), Chap. 9.
39. R. H. Lyddane, R. G. Sachs, and E. Teller, "On the polar vibrations of alkali halides," Phys. Rev. **59**, 673–676 (1941).
40. M. Born and K. Huang, *Dynamical Theory of Crystal Lattices* (Clarendon, 1954).